INL/CON-17-43116
PREPRINT

A Rejection Sampling Based Method for Determining Thermal Scattering Angle and Energy

M&C 2017 - International Conference on Mathematics & Computational Methods Applied to Nuclear Science & Engineering

Carl C. Haugen, Benoit Forget, Kord S. Smith

September 2017

The INL is a
U.S. Department of Energy
National Laboratory
operated by
Battelle Energy Alliance

M&C 2017 - International Conference on Mathematics & Computational Methods Applied to Nuclear Science & Engineering, Jeju, Korea, April 16-20, 2017, on USB (2017)

A Rejection Sampling Based Method for Determining Thermal Scattering Angle and Energy

Carl C. Haugen, Benoit Forget, Kord S. Smith

Massachusetts Institute of Technology, Boston, MA
cchaugen@mit.edu, bforget@mit.edu, kord@mit.edu

Abstract - *This paper proposes a new method for determining the outgoing energy and angle, E' and μ, of a thermal neutron after undergoing a scattering collision with a material. This method involves rejection sampling from the $\sqrt{E'} \cdot S(\alpha,\beta)$ kernel. While this new method is less computationally efficient than the old table lookup method, it has far lower data storage requirements, facilitates the treatment of temperature, provides a true continuous energy and angle representation, and enables the possibility of performing sensitivity analysis on fundamental thermal scattering parameters. This paper aims to demonstrate the feasibility of this approach leaving efficiency improvement to future work.*

I. INTRODUCTION

The field of computational reactor physics has traditionally relied heavily on deterministic models to simulate nuclear reactors. These deterministic methods often use empirical models to approximate underlying physics and rely on condensed multigroup cross sections. With continuing advancements in computational power, and an increasing desire to carry out high-fidelity, fully coupled multi-physics simulations, Monte Carlo methods are increasingly becoming the focus of method development for future applications. Monte Carlo methods have the advantage of being able to handle continuous energy cross sections and exact system geometry innately, so no approximations to the underlying physics are required. The major disadvantages associated with Monte Carlo methods are the comparatively high computational cost, and the high data storage requirements associated with reaction rate tallies on many regions and continuous energy cross sections at multiple system temperatures that are required for accurate interpolation.

Most high performance computing systems being deployed currently and envisioned for the future are based on making use of heavy parallelism across many computational nodes and many concurrent cores. These types of heavily parallel systems often have relatively little memory per core but large amounts of computing capability. This places a significant constraint on how data storage is handled in many Monte Carlo codes. This is made even more significant in fully coupled multiphysics simulations, which requires simulations of many physical phenomena be carried out concurrently on individual processing nodes, which further reduces the amount of memory available for storage of Monte Carlo data.

As such, there has been a move towards on-the-fly nuclear data generation to reduce memory requirements associated with interpolation between pre-generated large nuclear data tables for a selection of system temperatures. Methods have been previously developed and implemented in MIT's OpenMC Monte Carlo code for both the resolved resonance regime [1] and the unresolved resonance regime [2], but are currently absent for the thermal energy regime.

While data storage in the resolved and unresolved resonance regime has often been considered a larger limitation than in the thermal regime, this largely due to the fact that non-moderating materials have historically had their thermal neutron scattering data approximated with free gas scattering. In high fidelity models that aim to simulate all of the underlying physics in every materials, the thermal scattering data storage requirements are significant. As an example, for current treatment of the incoherent pathway for thermal neutron scattering in graphite, for every material temperature tabulated, for every incident neutron energy in the thermal scattering cross-section data, there will be 64 candidate scattered neutron energies and 1024 candidate scattering angles that need to be stored. Reducing this data storage requirement will facilitate accurate thermal scattering treatment of traditionally ignored materials (such as fuel and structural materials) in future simulations.

While there are many components involved in generating a thermal neutron scattering cross section on-the-fly, this work will focus on a proposed method for determining the energy and direction of a neutron after a thermal incoherent inelastic scattering event. This work proposes a rejection sampling based method using the thermal scattering kernel to determine the correct outgoing energy and angle. The goal of this project is to be able to treat the full $S(\alpha,\beta)$ kernel for graphite, to assist in high fidelity simulations of the TREAT reactor at Idaho National Laboratory. The method is, however, sufficiently general to be applicable in other thermal scattering materials, and can be initially validated with the continuous analytic free gas model.

II. THEORY

In order to generate thermal incoherent inelastic scattering data on-the-fly, a method is required for determining the energy of a neutron after a scattering event, E', as well as the scattering angle μ. The relationship between incoherent inelastic scattering and these two parameters is the double differential cross-section given by equation 1 for the symmetric definition of $\mathrm{S}(\alpha,\beta)$ [3].

$$\sigma(E \rightarrow E', \mu, T) = \frac{\sigma_{bound}}{2kT} \sqrt{\frac{E'}{E}} e^{-\frac{\beta}{2}} \mathrm{S}(\alpha,\beta) \qquad (1)$$

where $\mathrm{S}(\alpha,\beta)$ is the thermal scattering law parameter depending on the dimensionless momentum transfer parameter α and the dimensionless energy transfer parameter β.

$$\alpha = \frac{E + E' - 2\mu\sqrt{EE'}}{A_0 k_B T} \tag{2}$$

$$\beta = \frac{E' - E}{kT} \tag{3}$$

While cumulative probability distribution functions for both β and α can be computed via equations 4 and 5 [4], since these equations can not be analytically inverted, they can not be easily used in an on-the-fly methodology.

$$G(\beta|E,T) = \int_{\beta_{min}}^{\beta} e^{-\frac{\beta'}{2}} \frac{\int_{\alpha_{min}}^{\alpha_{max}} \mathrm{S}(\alpha,\beta',T)d\alpha}{\int_{\beta_{min}}^{\beta_{max}}\int_{\alpha_{min}}^{\alpha_{max}} e^{-\frac{\beta''}{2}}\mathrm{S}(\alpha,\beta'',T)d\alpha d\beta''} d\beta' \tag{4}$$

$$H(\alpha|\beta,E,T) = \int_{\alpha_{min}}^{\alpha} \frac{\mathrm{S}(\alpha',\beta,T)}{\int_{\alpha_{min}}^{\alpha_{max}} \mathrm{S}(\alpha'',\beta,T)d\alpha''} d\alpha' \tag{5}$$

We propose instead using the fact that the double differential cross section represents the probability of a given scattering path for an incident neutron, to use a rejection sampling scheme to determine E' and μ from $S(\alpha,\beta)$. Please note that for the remainder of this work, the asymmetric form of S [5], such that

$$S(\alpha,\beta) = e^{-\frac{\beta}{2}}\mathrm{S}(\alpha,\beta) \tag{6}$$

will be used. This changes the $\sqrt{\frac{E'}{E}}e^{-\frac{\beta}{2}}\mathrm{S}(\alpha,\beta)$ term in equation 1 to $\sqrt{\frac{E'}{E}}S(\alpha,\beta)$.

From equation 1, it can be determined that for a given incident energy E, the probability that any pair of outgoing energy E' and scattering angle μ will occur is

$$P(E',\mu) \propto \sqrt{E'} \cdot S(\alpha,\beta) \tag{7}$$

The simple rejection sampling scheme proposed in this work involves sampling E' uniformly from 0 to $E + 20k_BT$ and μ uniformly from -1 to 1. A random number is then sampled and checked against the ratio $\frac{\sqrt{E'}\cdot S(\alpha,\beta)}{sample\ limit}$. If the random number is less than this ratio, the candidate E' and μ values are accepted. The sampling limit is chosen such that it is above the highest possible value of $\sqrt{E'} \cdot S(\alpha,\beta)$ that will be seen for the material.

It is important to note that sampling uniformly in E' and μ is not equivalent to sampling uniformly in α and β. Since S is computed directly with the candidate values for α and β, it might seem more convenient to sample those values directly. However, this would require a non-constant sampling limit to preserve the correct scattering distribution. Instead of computing a new sampling limit for each candidate scattering event, it was determined that it was simpler to sample uniformly in E' and μ and calculate the corresponding α and β values.

For the thermal scattering kernels of real materials, the value of $S(\alpha,\beta)$ can be computed, using the Gaussian and incoherent approximations [5], from equation 8.

$$S(\alpha,\beta) = \frac{1}{2\pi}\int_{-\infty}^{\infty} e^{i\beta\hat{t}} \prod_j e^{-\left(\alpha\int_{-\infty}^{\infty}\frac{\rho_j(\beta')}{2;\beta'\cdot sinh\left(\frac{\beta'}{2}\right)}\left[1-e^{-i\beta' t}\right]e^{-\beta'/2}d\beta'\right)} d\hat{t} \tag{8}$$

In the case of simpler materials with little or no internal structure, the free gas model for $S(\alpha,\beta)$ can be used. This is demonstrated in equation 9.

$$S(\alpha,\beta) = \frac{1}{\sqrt{4\pi\alpha}} e^{-\left[\frac{(\alpha+\beta)^2}{4\alpha}\right]} \tag{9}$$

While figure 1 shows the total behaviour of $\sqrt{E'}S(\alpha,\beta)$ for an incident neutron energy of 0.7 eV, it is more informative to look at cross sections of its behaviour. Figures 2 and 3 present the function to be sampled for graphite with an incident neutron energy of $E = 0.7$ eV. Figure 2 shows how the function varies with β for a set value of α in graphite, while figure 3 shows how the function varies with α for a set value of β in graphite. The black line represents the $\sqrt{E'} \cdot S(\alpha,\beta)$ function that is being used for the rejection sampling, while the red line represents the rejection limit that is being used to check candidate alphas and betas.

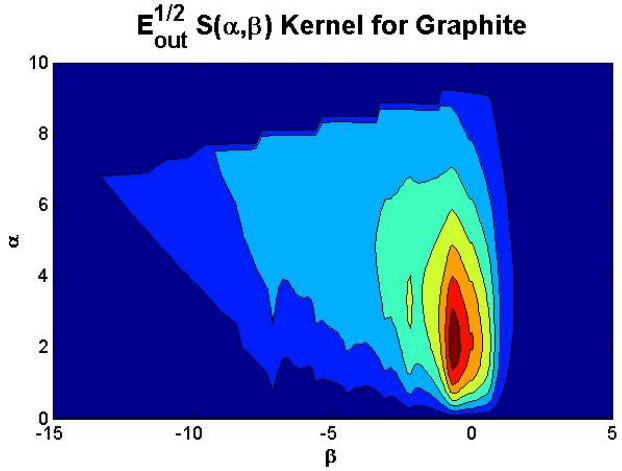

Fig. 1. Rejection Sampling Surface for 0.7 eV Neutron in Graphite

While in figure 2, the rejection surface does contain physically possible values for $\beta > 20$, the value of $\sqrt{E'} \cdot S(\alpha,\beta)$ continues to decrease in the steep exponential fashion. Since it has been used an the upper limit for numerical integration of $S(\alpha,\beta)$ in other work [4], $\beta = 20$ was the maximum upscatter value that was sampled in this method.

One of the major advantages of the rejection sampling scheme is that it allows for computation of continuous outgoing neutron energies and scattering angles, while many current libraries use an approximated discretized space. These libraries have tables of E' and μ for a grid of incident energies. When values of E' and μ are required, they are picked randomly from the tables (which are often set so that each of the values has an equal probability of being chosen), with no interpolation between the possible energies and angles. These are chosen such that, in principle, the average result over many

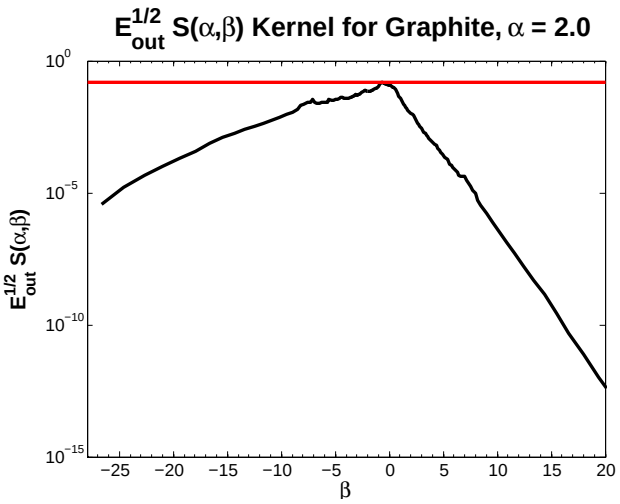

Fig. 2. Rejection Sampling Surface and Rejection Criteria for 0.7 eV Neutron in Graphite, β Dependence

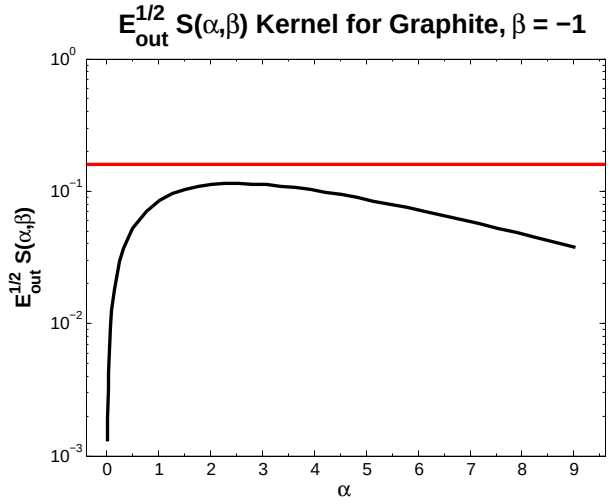

Fig. 3. Rejection Sampling Surface and Rejection Criteria for 0.7 eV Neutron in Graphite, α Dependence

neutrons should be identical to the correct result that would be obtained if a physical continuous model were being used. Recent extensions have proposed using a linearly interpolatable table in energy, as well as a smearing of the equiprobable bins in angle to provide a pseudo-continuous distribution in scattering angle [6], [7].

From figures 2 and 3, one obvious disadvantage can be seen with the current implementation of the rejection sampling algorithm. $\sqrt{E'} \cdot S(\alpha,\beta)$ varies by orders of magnitude in both α and β space, so there are many sampled values that have an extremely low probability of being accepted. This results in the rejection efficiency being very low, with many candidate α and β values needing to be tested to find the correct scattering distribution. This effect is even more pronounced in the free gas $S(\alpha,\beta)$ kernel, as shown in figures 4 and 5, where the value of S decays much more sharply in β. However, the free gas model is being used primarily for validation, so the efficiency of the rejection model with that $S(\alpha,\beta)$ kernel is less of a concern than the low efficiency with a real $S(\alpha,\beta)$ kernel. For example, it can be seen from figure 2, that if $\beta = -25$ is generated with $\alpha = 2$, the acceptance chance for this pair is on the order of 0.01%. A method for non-uniform weighted sampling of E' and μ so that a flat rejection limit is no longer required will be necessary for this rejection sampling scheme to be practical for use in large Monte Carlo simulations. The sampling efficiency could also be improved by reducing the maximum β value sampled. As can be seen from figure 2, this reduced limit could safely be used without much impact on the solution.

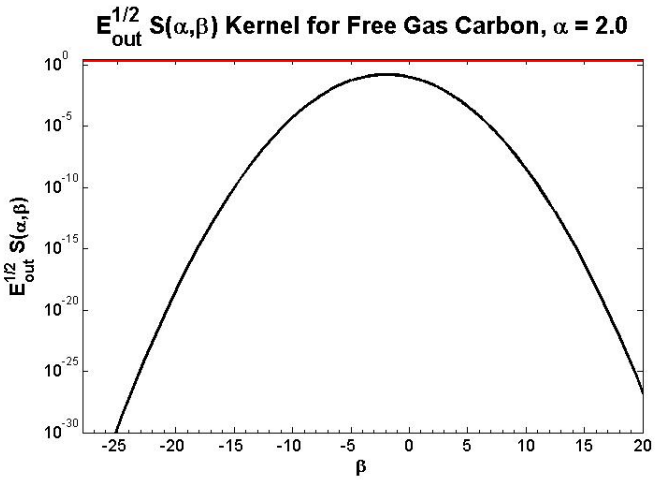

Fig. 4. Rejection Sampling Surface and Rejection Criteria for 0.7 eV Neutron in Free Gas Carbon, β Dependence

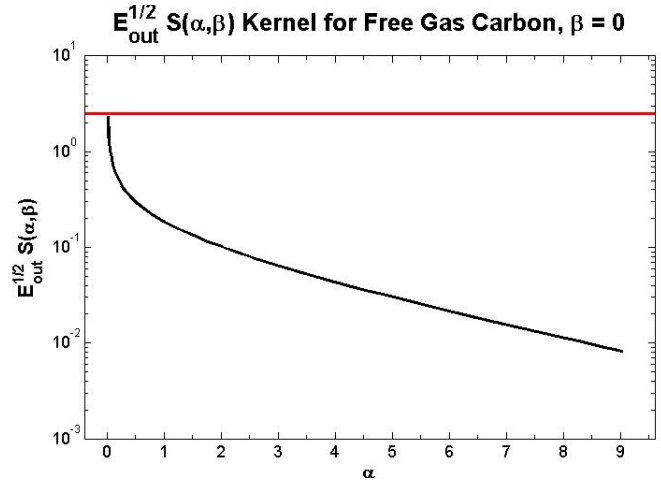

Fig. 5. Rejection Sampling Surface and Rejection Criteria for 0.7 eV Neutron in Free Gas Carbon, α Dependence

III. RESULTS AND ANALYSIS

The rejection sampling method for generating an outgoing energy and angle from a thermal scattering event appears able to reproduce the correct distribution of E' and μ.

This was initially tested by generating the probability distribution for scattering to all possible values of E' and μ using both the traditional method and with the new rejection sampling scheme discussed in this work. When comparing to free gas scattering in carbon, the rejection sampling scheme showed extremely good agreement at all tested temperatures and incident neutron energies. The agreement between the non-continuous traditional graphite scattering and continuous rejection graphite scattering is not perfect, but the overall behaviour is consistent. Plots of a representative selection of generated PDFs have been provided in an appendix at the end of this work.

The main comparison between the two methods that will be discussed in this work is the agreement between two benchmark problems.

A fixed source calculation was carried out on a simple heavy scattering problem to determine accuracy of the method. This system was a large pure carbon block, infinite in the z direction, and a 1.4 $m \times 1.4$ m square in the $x-y$ plane. The source neutrons were populated in a 2 $cm \times 2$ cm square in the middle of the problem from the χ spectrum with random initial angular distribution. A second simulation was carried out on a simplified model of the Idaho National Lab TREAT reactor core. This is an eigenvalue calculation of a system that is >99% graphite by mass. Both of these simulation problems are dominated by scattering in graphite, which lend themselves to testing a thermal scattering model. While common practice requires the use of $S(\alpha,\beta)$ tables for graphite, we are using the free gas thermal scattering model for testing purposes because it is continuous, which allows direct comparison with the rejection sampling scheme.

The primary metrics for the fixed source scattering in the graphite block were the agreement between the neutron leakage fraction out of the slab and the thermal flux distribution in the slab. In the simplified TREAT core eigenvalue problem, the metrics examined were the core eigenvalues and the leakage fraction exiting the graphite reflector region surrounding the core (combined axial and radial leakage).

1. Free Gas Model

The most basic model to test the accuracy of the rejection sampling methodology is to use the free gas model for the carbon $S(\alpha,\beta)$. The free gas model has advantages of having a simple and inexpensive definition of S, and that the traditional sampling algorithm generates continuous distributions in E' and μ. The continuous nature of scattering distributions generated by the traditional method provides an easy method of validation for the continuous results generated by the rejection method. It should be noted that the intent of this work was never to replace the free gas method of scattering, since there would be little benefit to doing so, while there would be a significant sacrifice of computational efficiency.

Table I shows the results obtained from simulating carbon scattering both with the free gas rejection model and with the traditional free gas scattering model used in OpenMC [8] for the fixed source carbon scattering problem.

The agreement between the traditional model for computing E' and μ is very good, agreeing within the ± 95% confidence intervals in almost all metrics examined.

The simplified TREAT core was also simulated using free gas carbon data, both with the traditional scattering model, and the rejection sampling model. Table II shows that this simulation also agreed very well within the 95% confidence intervals for all metrics.

The efficiency of this rejection scheme is currently very low, often requiring hundreds to thousands of sampling attempts to find a valid E' and μ pair at each scattering event. While the sampling efficiency will be improved in future work, the goal of this sampling scheme was never to replace the traditional free gas scattering model but simply to use it for verification.

2. Full Graphite $S(\alpha,\beta)$

The second model that was tested was the same fixed source slab and simplified TREAT reactor problems using the full graphite $S(\alpha,\beta)$ to inform the cross sections and scattering E' / μ values. The $S(\alpha,\beta)$ values used for this test were interpolated from a pre-computed table. This was done largely to prevent the addition of large additional cost from direct calculation of $S(\alpha,\beta)$ in this scoping study. Unlike the free gas $S(\alpha,\beta)$ kernel, the thermal scattering kernel generated by using the phonon spectrum of a real material is non-trivial to compute. This does, however, mean that the $S(\alpha,\beta)$ values being used were not truly continuous. As an added layer of complexity, most traditional thermal scattering libraries use discrete values of equiprobable E' and μ, while the rejection method selects from a continuous spectrum in E' and μ (a more faithful representation of the physics), making it is more difficult to draw conclusions from comparison between the two methods. Table III shows that there are significant differences between the scattering results of the continuous rejection scattering in this proposed method and the methodology used by most reactor physics data libraries for the graphite block benchmark. For this comparison, a tabular sampling method containing 64 equiprobable values of E' and 16 equiprobable values of μ for each incident E was used (this is the type of scattering used by libraries such as NNDC and JEFF). There is no interpolation between these values - it is typically assumed that the integrated result over many neutrons will probabilistically converge to the correct result. To show how large an impact this discretization has on the result, another simulation, using tabular interpolation to determine E' from a grid of points, and setting μ to one of a set number of possible (equiprobable, non-interpolated) values, was carried out. This is a better methodology than using equiprobable bins for both parameters [7]. For this simulation, for each value of E in the data table, 1024 E' interpolation points and 32 equiprobable μ bins were used. These results are reported in table III.

These tests show that higher discretization brings most of the metrics closer to the values observed in the continuous rejection sampling case, but not by enough to draw a definitive conclusion.

Similarly, when comparing the results of the rejection sampling scheme using the graphite $S(\alpha,\beta)$ kernel to the results of the simulation with the tabulated 64 equiprobable E' and 16 equiprobable μ values, there are significant differences

Computed Parameter	Traditional Method Result	Traditional Method Confidence Interval	Rejection Method Result	Rejection Method Confidence Interval
Leakage Fraction	0.70351	0.00139	0.70303	0.00152
Flux < 0.005 eV	17.2514	0.056894	17.2106	0.059856
Flux 0.005 - 0.01 eV	43.5058	0.148507	43.4048	0.139925
Flux 0.01 - 0.05 eV	536.923	1.70650	536.102	1.39021
Flux 0.05 - 0.1 eV	332.177	1.12617	331.905	0.996793
Flux 0.1 - 0.5 eV	129.488	0.383167	129.583	0.320090
Flux 0.5 - 1.0 eV	11.5805	0.023418	11.6489	0.023472
Flux 1.0 - 5.0 eV	25.5816	0.033438	25.7569	0.032811

TABLE I. Agreement Between Rejection Sampling Method and Traditional Method for Free Gas Carbon in Fixed Source Scattering

Computed Parameter	Traditional Method Result	Traditional Method Confidence Interval	Rejection Method Result	Rejection Method Confidence Interval
k_{eff} (Collision)	1.07040	0.00312	1.07115	0.00358
k_{eff} (Track-Length)	1.07029	0.00319	1.07113	0.00356
k_{eff} (Absorption)	1.06998	0.00235	1.06979	0.00294
Combined k_{eff}	1.07031	0.00190	1.06989	0.00223
Leakage Fraction	0.04670	0.00050	0.04711	0.00045

TABLE II. Agreement Between Rejection Sampling Method and Traditional Method for Free Gas Carbon in a Simplified TREAT Eigenvalue Problem

between the computed eigenvalues and core leakage fractions that are not sufficiently accounted for by the simulation uncertainties. The results of these simulations can be seen in table IV.

3. Rejection Efficiency

As discussed previously in this work, one of the major difficulties encountered with the simplified version of the rejection sampling method proposed here is that it has a very low rejection efficiency. Due to the sampling surface varying by orders of magnitude (see figures 2 and 3), most candidate E' and μ values are not accepted. Table V shows the computational times for the benchmark problems discussed above. It is important to note that these are times for the entire simulation, and while the test problems are heavily thermal, some of the computational time is spent on slowing down through the higher energy regimes, and on non-scattering interactions.

The increase in computational cost is more than two orders of magnitude in the heavily scattering pure graphite system when going from the traditional methods to the rejection sampling schemes. In a system closer to a nuclear power reactor, where fissile isotopes are present, the increase in computational cost is much less, but still on the order of 5 - 50 ×.

It can be seen from figures 6 and 7 that the simple rejection sampling algorithm can take hundreds to thousands of attempts to find a valid E' and μ pair for each thermal neutron scattering event. This is prohibitive for use in production level Monte Carlo codes.

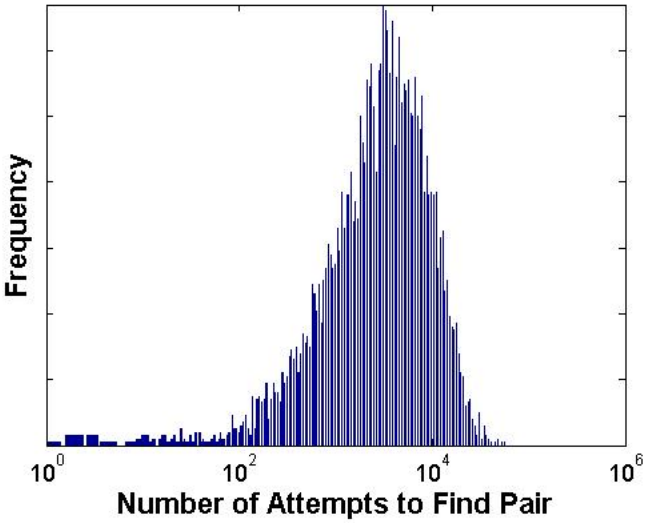

Fig. 6. Distribution of Number of Attempts Required to Find a Valid α / β Pair for Free Gas Rejection Sampling

For this reason, in order for this rejection sampling scheme to be practical in the future, a sampling bias must be introduced to allow the method to move away from uniformly sampling in E' and μ so that a non-constant rejection

Computed Parameter	Rejection Method Result	Rejection Method Confidence Interval	64 Discrete E' 16 Discrete μ Result	64 Discrete E' 16 Discrete μ Confidence Interval	Interpolated E' 32 Discrete μ Result	Interpolated E' 32 Discrete μ Confidence Interval
Leakage Fraction	0.70505	0.00116	0.70940	0.00162	0.70771	0.00110
Flux < 0.005 eV	16.6714	0.157206	15.3995	0.077969	15.5073	0.127739
Flux 0.005 - 0.01 eV	42.8473	0.229711	35.7861	0.219346	40.5120	0.252109
Flux 0.01 - 0.05 eV	532.998	1.79710	524.695	1.36235	521.517	1.52923
Flux 0.05 - 0.1 eV	334.134	0.995411	342.045	0.781433	341.221	1.02381
Flux 0.1 - 0.5 eV	140.564	0.348048	148.839	0.342259	148.633	0.336976
Flux 0.5 - 1.0 eV	12.0581	0.027606	12.8352	0.017330	12.8009	0.027009
Flux 1.0 - 5.0 eV	25.1700	0.028748	26.5651	0.020209	26.5582	0.036654

TABLE III. Agreement Between Rejection Sampling Method and Tabular Methods for Graphite Carbon, Fixed Source Scattering

Computed Parameter	Traditional Method Result	Traditional Method Confidence Interval	Rejection Method Result	Rejection Method Confidence Interval
k_{eff} (Collision)	1.04850	0.00200	1.05692	0.00278
k_{eff} (Track-Length)	1.04853	0.00195	1.05725	0.00279
k_{eff} (Absorption)	1.05236	0.00281	1.06157	0.00149
Combined k_{eff}	1.04936	0.00216	1.06126	0.00183
Leakage Fraction	0.05057	0.00044	0.04729	0.00026

TABLE IV. Agreement Between Rejection Sampling Method and Traditional Method for Graphites Carbon in a Simplified TREAT Eigenvalue Problem

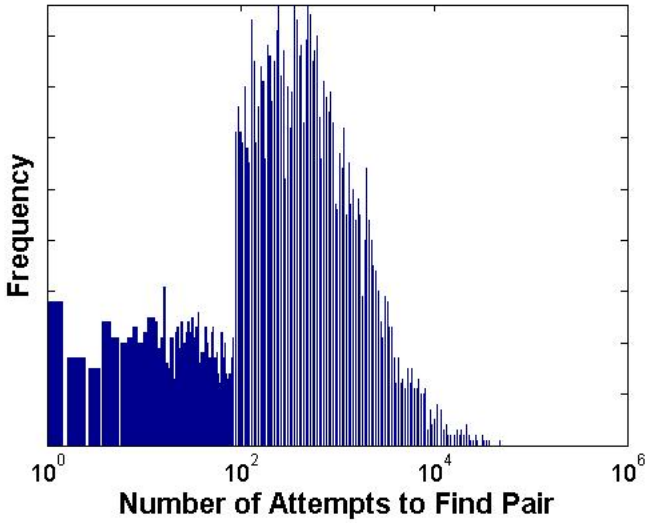

Fig. 7. Distribution of Number of Attempts Required to Find a Valid α / β Pair for Graphite Rejection Sampling

limit can be used. One of the potentially simplest changes that could be made would be to sample over integrated ranges of α and β values, each with different upper rejection limits, or by bounding the kernel by a simple function that more closely follows the physics and is analytically inverted.

IV. CONCLUSIONS AND FUTURE WORK

The use of a rejection sampling scheme to determine E' and μ of a neutron after an incoherent inelastic thermal scattering collision has been shown to reproduce the results seen using traditional methods for the analytic free gas case, both in fixed source and eigenvalue simulations. This demonstrates the validity of the method.

The rejection sampling scheme does not currently obtain the exact same results as the approximated discrete models for handling full $S(\alpha,\beta)$ kernels in materials (such as graphite). This could arise from the interpolation of $S(\alpha,\beta)$ in the current implementation of the rejection sampling algorithm instead of being purely continuous. This is a concern primarily because of the pseudo-exponential decay of the $S(\alpha,\beta)$ kernel, which results in an incorrect interpolation scheme having the potential to generate a $S(\alpha,\beta)$ that is too far off from the true value to preserve the correct physics. Additionally, previous work at LANL [7] has shown that the compounding effect of the discrete equiprobable angles and energies used in the traditional $S(\alpha,\beta)$ treatment can lead to unphysical anomalies, suggesting that the reference solutions might be slightly different from what would be obtained by perfectly adhering to all the underlying physics. More work will be done to demonstrate that the rejection sampling model is valid for complex $S(\alpha,\beta)$ kernels as well.

Using a flat rejection limit and uniformly sampling in E' and μ has resulted in a rejection sampling scheme that works

Problem	$S(\alpha,\beta)$ Definition	Traditional Method Time (s)	Rejection Method Time (s)	Computational Cost Increase
Graphite Block	Free Gas	251.44	58651	233×
Simplified TREAT	Free Gas	1255.6	56127	44.7 ×
Graphite Block	Graphite $S(\alpha,\beta)$	169.35	20694	122×
Simplified TREAT	Graphite $S(\alpha,\beta)$	552.09	2605.5	4.72×

TABLE V. Computational Time Increase from Using Simple Rejection

but is very inefficient. This is due to the fact that the rejection surface varies by orders of magnitude over the sampling range. Further work will be carried out to improve the efficiency of this scheme, so that it will be an effective method for use in Monte Carlo applications.

V. ACKNOWLEDGMENTS

This work was funded by the Idaho National Laboratory, which is supported by the Office of Nuclear Energy of the U.S. Department of Energy under Contract No. DE-AC07-05ID14517.

REFERENCES

1. C. JOSEY, P. DUCRU, B. FORGET, and K. S. SMITH, "Windowed Multipole for Cross-Section Doppler Broadening," *Journal of Computational Physics*, **307**, 715–727 (2016).
2. J. A. WALSH, B. FORGET, K. S. SMITH, and F. B. BROWN, "On-the-Fly Doppler Broadening of Unresolved Resonance Region Cross-Sections via Probability Band Interpolation," *PHYSOR* (2016).
3. F. G. BISCHOFF, M. L. YEATER, and W. E. MOORE, "Monte Carlo Evaluation of Multiple Scattering and Resolution Effects in Double-Differential Scattering Cross-Section Measurements," *Nuclear Science and Engineering*, **48**, 266–270 (1972).
4. A. T. PAVLOU and W. JI, "On-the-Fly Sampling of Temperature-Dependent Thermal Neutron Scattering Data for Monte Carlo Simulations," *Annals of Nuclear Energy*, **71**, 411–426 (2014).
5. R. E. MACFARLANE, "The NJOY Nuclear Data Processing System," Tech. Rep. LA-UR-12-27079, Los Alamos National Laboratory (2012).
6. A. T. PAVLOU, F. B. BROWN, W. R. MARTIN, and B. C. KIEDROWSKI, "Comparison of Discrete and Continuous Thermal Neutron Scattering Cross-Section Treatments in MCNP5," , *LA-UR-11-04542* (2011).
7. J. L. CONLIN, D. K. PARSONS, F. B. BROWN, R. E. MACFARLANE, R. C. LITTLE, and M. C. WHITE, "Continuous-S(alpha,beta) Capability in MCNP," *Transactions of the American Nuclear Society*, **106**, *LA-UR-12-00155* (2012).
8. E. M. GELBARD, "Epithermal Scattering in VIM," Tech. Rep. FRA-TM-123, Argonne National Laboratory (1979).

APPENDIX

The first test of the validity of the rejection sampling scheme involved generating probability distributions in E' and μ for a number of incident neutron energies and material temperatures using both the traditional method and with the new rejection sampling scheme. As mentioned previously in this work, when comparing to free gas scattering in carbon, the rejection sampling scheme showed extremely good agreement at all tested temperatures and incident neutron energies. The agreement between the non-continuous traditional graphite scattering and continuous rejection graphite scattering is not perfect, but the overall behaviour is consistent. Plots of a representative selection of generated PDFs are shown with the figures 8 to 15.

Note that the E' values on the x-axes in all figures in this section are given in MeV.

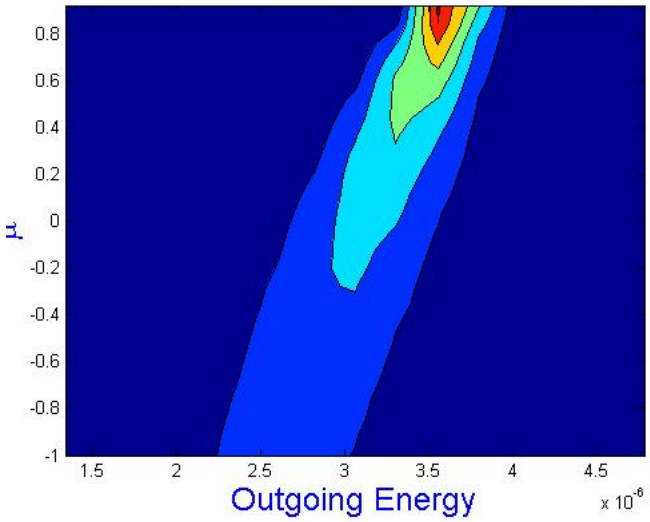

Fig. 8. E' / μ Distribution Generated by a 3.8 eV Neutron Scattering in Free Gas Carbon at 1200 K, Using the Traditional Method

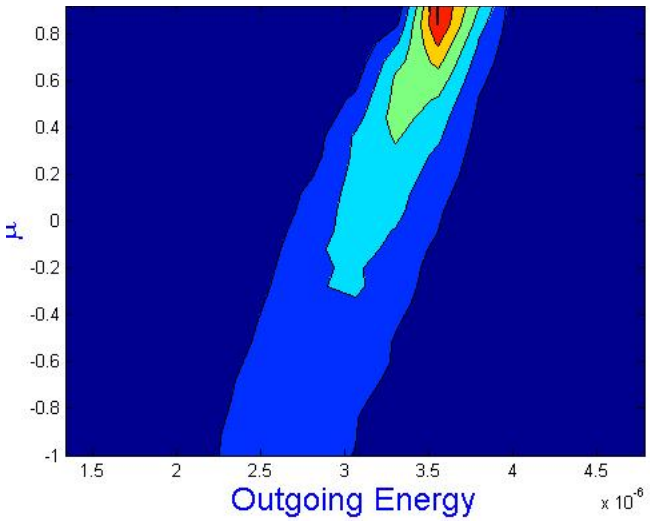

Fig. 9. E' / μ Distribution Generated by a 3.8 eV Neutron Scattering in Free Gas Carbon at 1200 K, Using the Rejection Method

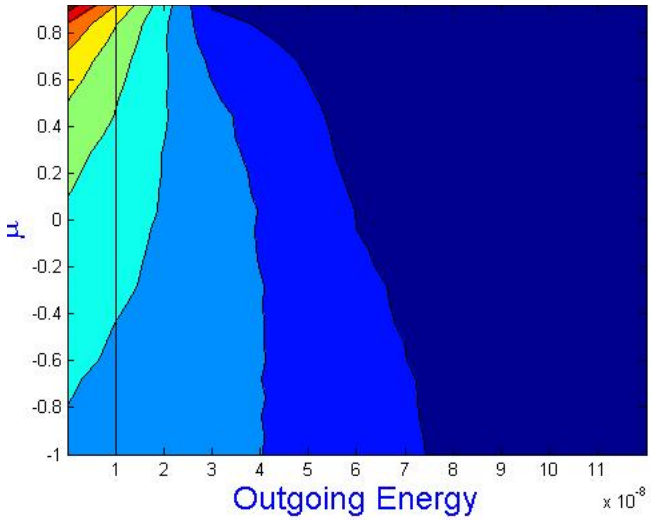

Fig. 10. E' / μ Distribution Generated by a 10 meV Neutron Scattering in Free Gas Carbon at 1200 K, Using the Traditional Method

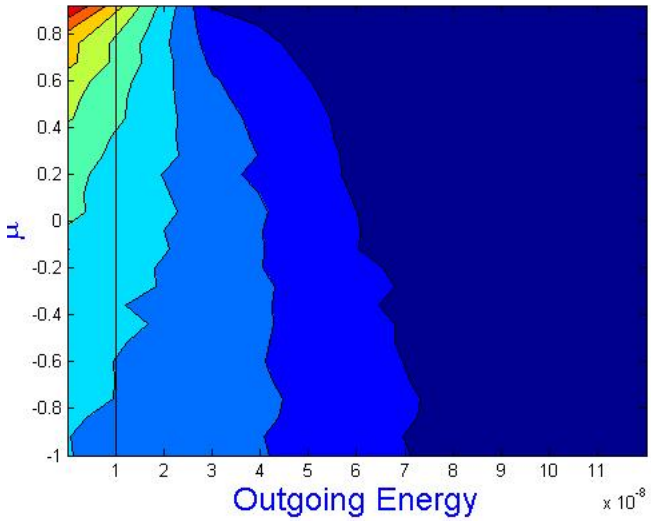

Fig. 11. E' / μ Distribution Generated by a 10 meV Neutron Scattering in Free Gas Carbon at 1200 K, Using the Rejection Method

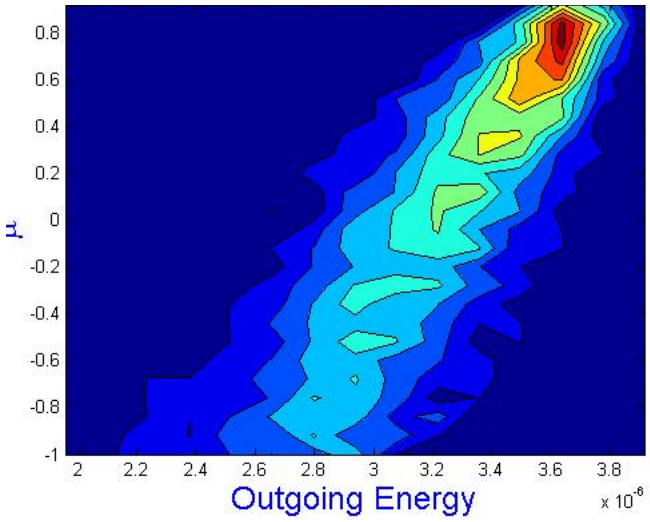

Fig. 12. E' / μ Distribution Generated by a 3.8 eV Neutron Scattering in Graphite Carbon at 293 K, Using the Traditional Method

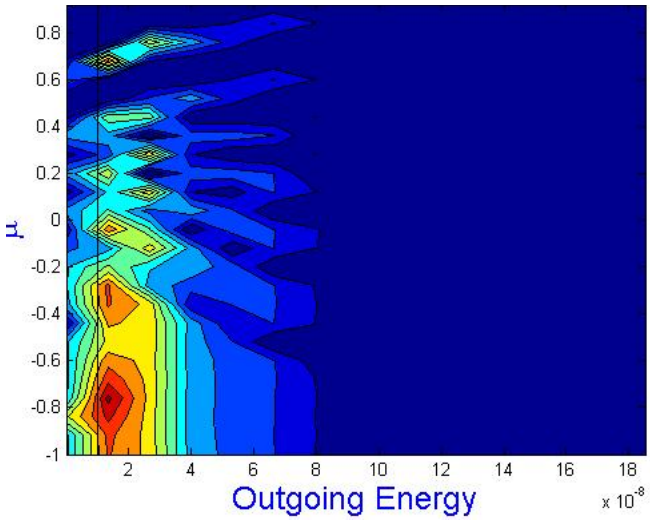

Fig. 14. E' / μ Distribution Generated by a 10 meV Neutron Scattering in Graphite Carbon at 293 K, Using the Traditional Method

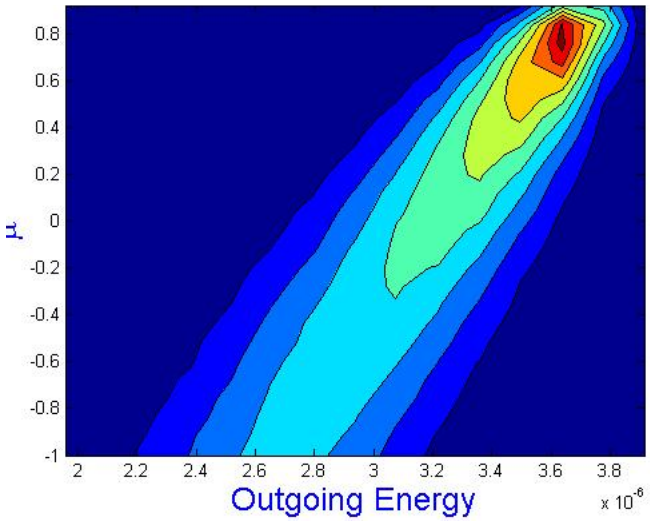

Fig. 13. E' / μ Distribution Generated by a 3.8 eV Neutron Scattering in Graphite Carbon at 293 K, Using the Rejection Method

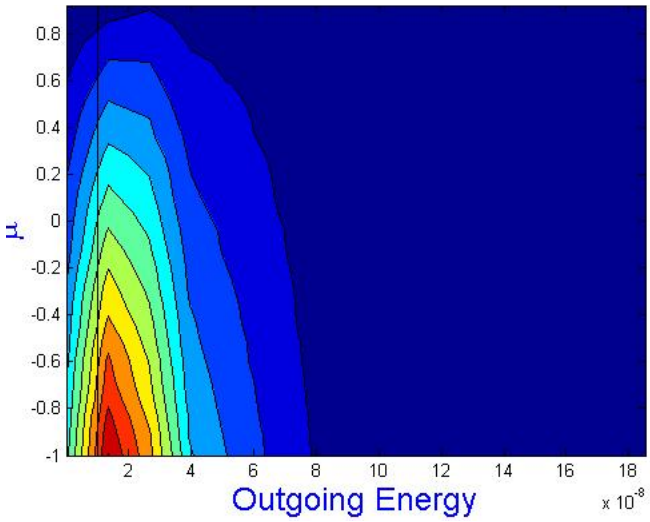

Fig. 15. E' / μ Distribution Generated by a 10 meV Neutron Scattering in Graphite Carbon at 293 K, Using the Rejection Method